

Received March 31, 2020, accepted April 16, 2020, date of publication April 29, 2020, date of current version May 18, 2020.

Digital Object Identifier 10.1109/ACCESS.2020.2991197

# Multiobjective Optimization of Uplink NOMA-Enabled Vehicle-to-Infrastructure Communication

WALI ULLAH KHAN<sup>1</sup>, (Student Member, IEEE), FURQAN JAMEEL<sup>2</sup>,  
GUFTAAR AHMAD SARDAR SIDHU<sup>3</sup>, MANZOOR AHMED<sup>4</sup>,  
XINGWANG LI<sup>5</sup>, (Senior Member, IEEE), AND RIKU JÄNTTI<sup>2</sup>

<sup>1</sup>School of Information Science and Engineering, Shandong University, Qingdao 266237, China

<sup>2</sup>Department of Communications and Networking, Aalto University, 02150 Espoo, Finland

<sup>3</sup>Department of Electrical and Computer Engineering, COMSATS University Islamabad, Islamabad 44000, Pakistan

<sup>4</sup>Department of Computer Science and Technology, Qingdao University, Qingdao 266071, China

<sup>5</sup>School of Physical and Electronics Engineering, Henan Polytechnic University, Jiaozuo 454003, China

Corresponding author: Manzoor Ahmed (manzoor.achakzai@gmail.com)

This work was supported in part by the National Key Research and Development Plan Key Special Projects under Grant 2018YFB2100303, in part by the Shandong Province Colleges and Universities Youth Innovation Technology Plan Innovation Team Project under Grant 2020KJN011, and in part by the Program for Innovative Postdoctoral Talents in Shandong Province under Grant 40618030001. The work of Furqan Jameel and Riku Jäntti was supported in part by the 5G-MOBIX Project funded by the European Unions Horizon 2020 Research and Innovation Programme under Grant 825496.

**ABSTRACT** Vehicular communication is gradually evolving from the rudimentary data exchange techniques to innovative, efficient, and large-scale communication platform. The future vehicular networks aim to offer new services and achieve massive connectivity with the aid of advanced wireless communication techniques. In this regard, one of the emerging paradigms is non-orthogonal multiple access (NOMA) which holds the promise to meet the resource-intensive demands of future networks. Due to this reason, the applications of NOMA are being investigated by the researcher of academia and industry alike. This article aims to build on the state-of-the-art by providing a novel multiobjective optimization framework for vehicle-to-infrastructure (V2I) communications. Specifically, this work aims to improve upon the sum-rate and energy efficiency of uplink NOMA-enabled V2I communications. The formulated problem is based on the tradeoff between sum-rate and total transmit power while maintaining the quality of service (QoS) requirements of the network. To provide a reliable solution, a multiobjective optimization framework has been proposed by applying the weighted-sum method and handle joint metrics of sum-rate maximization and total transmit power minimization. Extensive simulations have been performed to validate the superiority of the proposed framework against conventional benchmark techniques. The results clearly indicate that the proposed framework is feasible for NOMA-enabled V2I communication and can be scaled up for practical implementation.

**INDEX TERMS** Non-orthogonal multiple access, multiobjective optimization, QoS, vehicular communication.

## I. INTRODUCTION

Recent years have seen tremendous growth in terms of research interest in vehicular communications [1]. This is partly due to the fascination of the research community with autonomous vehicles and utility in road safety applications. To materialize the concept of the fully autonomous trans-

The associate editor coordinating the review of this manuscript and approving it for publication was Rentao Gu<sup>id</sup>.

portation system, it is deemed necessary to build an efficient and reliable communication network among vehicles and other roadside entities. For these realizations, there generally exist two distinct communication regimes, i.e., dedicated short-range communications (DSRC) and cellular vehicular (C-V2X) communications [2]. Both regimes have been proven to be useful under different circumstances and communication requirements. The DSRC approach for vehicular communication is useful for enabling connectivity in

ad-hoc vehicular networks, whereas, the C-V2X communication takes advantage of the cellular network for establishing long-range links among vehicles. This work mainly focuses on the uplink part of C-V2X communication due to its ability to incorporate a large number of vehicles in the network.

In general, there are two modes of communication in C-V2V, namely the direct communications (DC) and network-based communications (NC) modes. For the DC mode, the vehicles are able to directly communicate with each other, whereas, NC mode exploits the role of the cellular base station (BS) or roadside unit (RSU) in assisting communication among vehicles [3]. However, it has been observed that the current communication architecture is unable to scale up with the increasing number of vehicles on the road. Since orthogonality is one of the necessities of the present networks, it is very likely that the mobile (i.e., vehicles) and static users cannot be served with varying transmit rates and improved quality of service (QoS). Due to the ever-present constraint of spectral resources, non-orthogonal multiple access (NOMA) has attracted the interest of researchers as an alternative to orthogonal multiple access (OMA) [4], [5]. Using the power variations at the transmitter side, NOMA supports multiple users over the same spectrum resource [6]. Then, the successive interference cancellation (SIC) is used at the receiver side to decode different signals [7]. Moreover, since NOMA is inherently immune to the effect of carrier frequency offset (CFO), it is considered as one of the promising solutions for vehicular communications [1]. This article mainly explores the utility of NOMA in vehicular communications and its feasibility for mitigating the spectrum bottleneck of such networks.

#### A. RECENT WORKS

Recently, there exist several studies in the literature on NOMA-enabled vehicular communication networks. For vehicular-to-everything (V2X) networks [8], Di *et al.* proposed scheduling and resource allocation problems to reduce latency and improve the reliability of the NOMA-enabled system. The authors first provided centralized semi-persistent scheduling for transmitter-receiver selection and sub-channel allocation. And then distributed scheme for power allocation was exploited. The same authors in [9] further extended the work by proposing both resource allocation and power control schemes. By employing matching theory, here, the BS performed semi-persistent scheduling and sub-channel allocation in a centralized way. Then, by using iterative signaling control, the vehicles autonomously calculated the power management in a distributed manner. In [10], Xiao *et al.* proposed a dynamic vehicle clustering and power management scheme for the NOMA-enabled V2X systems. The authors' system model was composed of a single BS and multiple vehicle clusters, and the objective was to enhance the minimum achievable rate of the vehicles. To mitigate interference and increase the sum rate, the authors of [11] investigated a resource allocation problem in device-to-device (D2D)-enhanced V2X NOMA networks. Moreover,

they proposed a greedy algorithm based on a hyper-graph three-dimension (3D) matching algorithm to solve the interference mitigation resource management problem. The same authors presented three-partite (3P) to model the complex interference environment and then employed an interference hyper-graph 3D matching resource management scheme based on greedy and iterative algorithms.

By considering a road junction scenario where the vehicles at cross-road junction have very similar channel gains and the NOMA technique is difficult to apply, the work of [12] proposed two-channel gain stretching strategies to artificially generate channel gain difference among different vehicles on the same spectrum resource. The authors then derived a closed-form expression for the outage probability, where the NOMA-enabled V2X system outperformed the conventional OMA-enabled system. References [13] and [14] applied a centralized resource allocation scheme to improve the sum rate of D2D-enhanced V2X NOMA networks. The authors first constructed an interference hypergraph to model interference environment and, based on this constructed hypergraph model, a cluster coloring algorithm for interference hyper-graph resource management scheme was investigated. Guo and Zhou [15] studied a power control problem in NOMA-enabled heterogeneous vehicular networks to improve spectral efficiency and reliability. By considering the imperfect channel estimation, the authors formulated a chance-constrained optimization problem to enhance the uplink transmission rate of the vehicular network. Moreover, the chance constraints were first transformed into deterministic constraints and then they derived the corresponding feasible region and optimal solution. The same authors in [16] modified the work of [15] by considering joint spectrum and power allocation in heterogeneous vehicular networks. They first decouple the resource management problem for channel assignment and power control subproblems and then designed a cascaded Hungarian algorithm for efficient channel allocation. Later, for assigned channels, the authors used an approximation to transform the chance constraints into deterministic constraints and accordingly obtain the optimal solution. In [17], the power allocation scheme based on vehicle mobility was proposed in NOMA-enabled uplink vehicular-to-infrastructure (V2I) systems. The goal was to reduce the bit error rate and increase the spectral efficiency under the Rayleigh fading channels.

A joint framework of cell association and power control for the vehicle-to-small-cell (V2S) network was investigated in [18]. The authors' aim was to enhance the system's long-term performance and to reduce the number of handovers. By employing the gradient scheduling method, the optimization problem was first transformed to per time frame weighted sum-rate maximization problem and then a hierarchical power control algorithm was adopted based on Karush-Kuhn-Tucker (KKT) conditions and successive convex approximation to obtain the optimal solutions. Xu and Gu [19] studied the resource management problem in the NOMA-enabled vehicle-to-vehicle (V2V) network.

They solved the NP-hard problem using a centralized resource management algorithm and their objective was to optimize the packet receive ratio. The same authors in [20] extended the work of V2V as discussed in [19] by considering multiple-input multiple-output and special modulation techniques. Here, the target was to optimize spectrum efficiency and the bit error rate of the NOMA-enabled V2V system. The power control problems for achievable rate maximization were proposed in NOMA-enabled V2X broadcasting and multicasting systems [21]. To obtain efficient solutions, they employed bisection methods to handle quasi-concave power optimization problems. A resource allocation problem for the V2X network [22] where cellular users max-min rate fairness and vehicular users minimum signal-to-interference-plus-noise ratios (SINRs) were considered. The authors first decouple the optimization problem into three subproblems, and then the Perron-Frobenius theorem, Kuhn-Munkres algorithm, and matching theory were exploited to obtain efficient solutions. Of late, Zhang *et al.* [23] provided a full-duplex decentralized NOMA-enabled V2X system. The authors considered both urban and suburban scenarios, where the objectives were to enhance the system capacity. To tackle the non-convex problem in both scenarios, the authors derived the closed-form expression for efficient solutions.

## B. MOTIVATION AND CONTRIBUTIONS

Although a substantial amount of work has already been done on NOMA-enabled vehicular communications, the tradeoff between rate and transmit power of these networks is not well understood. To date, most of the studies on vehicular communications have focused on single-objective optimization, such as optimizing spectral efficiency and energy efficiency. However, in practice, the system parameters are dependent on each other and optimizing one function may lead to degradation of the other. Thus, it is more desirable to optimize more than one function with different objectives, which raises the requirement of multiobjective optimization [24]. To the best of the authors' knowledge, the multiobjective optimization aspect of NOMA-enabled vehicular networks has not been explored yet due to the associated complexity in analysis. Thus, with the intent to provide novel insights on these matters, this article presents a novel framework for optimizing the tradeoff between the sum-rate and total transmit power of the NOMA-enabled vehicular networks. The main contributions of our work are summarized as follows:

- 1) We develop an uplink NOMA-enabled V2I communication network and formulate a problem keeping in view the QoS constraints of such networks. These constraints include the achievable rate and battery power of the vehicles.
- 2) Based on the formulated problem, detailed insights have been provided on the tradeoff between sum-rate and total transmit power of uplink NOMA-enabled V2I networks.
- 3) To optimize this tradeoff, a multiobjective optimization framework has been proposed. The superiority of the

**TABLE 1. The list of different symbols and their definitions.**

No.	Symbol	Definition
1.	$\mathcal{V}$	Set of mobile vehicles in the network
2.	$V_j$	Indicate mobile vehicle $j$
3.	$y_j$	Received signal at $V_j$
4.	$g_j$	Channel gain of $V_j$
5.	$p_j$	Transmit power of $V_j$
6.	$z_j$	signal of $V_j$
7.	$N_j$	Additive white Gaussian noise of $V_j$
8.	$\sigma^2$	Variance of additive white Gaussian noise
9.	$R_j$	Data rate of $V_j$
10.	$\gamma_j$	SINR of $V_j$
11.	$\beta$	Gap among vehicles power for efficient SIC
12.	$R_{min}$	Minimum threshold of QoS requirements
13.	$itr$	Indicate iteration number
14.	$\lambda_j$	Lagrangian multiplier/dual variable
15.	$\mu_j$	Lagrangian multiplier/dual variable
16.	$\eta_j$	Lagrangian multiplier/dual variable
17.	$L$	Lagrangian function
18.	$D$	Dual problem
19.	$\omega$	Step size
20.	$\rho_j$	Binary variable for vehicle selection

proposed multiobjective solution has been shown via comparison with a benchmark single objective optimization solution.

## C. ORGANIZATION

The rest of the article is organized as follows. Section II depicts the system model and provides problem formulation steps. Section III presents the proposed multiobjective based solution. In Section IV, the numerical results and discussion are provided. Finally, Section V provides concluding remarks and future research directions. A list of definitions of commonly used symbols is provided in Table 1.

## II. SYSTEM MODEL AND PROBLEM FORMULATION

This section provides the details of the considered system model and, subsequently, discusses the problem formulation procedure.

### A. SYSTEM MODEL

We consider an uplink transmission of the NOMA-enabled vehicular communication network as depicted in Fig. 1. Our considered scenario consists of a single RSU and  $J$  mobile vehicles, where  $\mathcal{V} = \{V_j | j = 1, 2, 3, \dots, J\}$ . All vehicles are multiplexed on the same spectrum resource at the same time by using power multiplexing NOMA. The RSU and mobile vehicles are assumed to equip with a single antenna. Since the mobile vehicles are associated with the RSU, we consider that RSU has the knowledge of channel state information (CSI) of all the mobile vehicles.<sup>1</sup> Moreover, we assume that the

<sup>1</sup>Following the approach of [25], [26], we have not considered the mobility of the vehicles on the road. By considering the mobility of the vehicles, the channel characteristics and the CSI estimation of vehicles are expected to vary leading to different admission control policies and vehicle associations. Since our main objective is to optimize the energy and spectral efficiencies, the issues pertaining to imperfect CSI and fast fading would be considered in future studies.

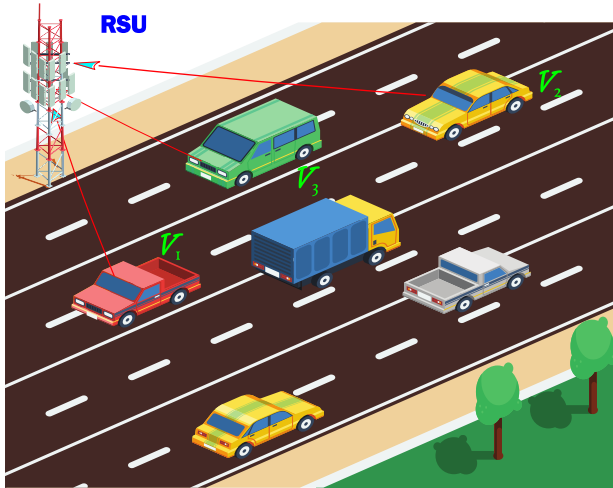


FIGURE 1. An illustration of system model.

wireless channels between RSU and its associated mobile vehicles follow Nakagami- $m$  fading [27]. Without loss of generality, we sort the channel gains of mobile vehicles as<sup>2</sup>  $|g_1| \leq |g_2| \leq \dots \leq |g_j| \leq \dots \leq |g_J|$ . Different from the downlink NOMA where the nearest mobile vehicle (the one with strongest channel quality) can detect and subtract the signal of far mobile vehicle (the one with weak channel quality), in uplink NOMA, the RSU will not apply SIC for near mobile vehicle and decodes it with the interference of far mobile vehicle while the RSU apply SIC for far mobile vehicle, subtract all other vehicles' signals and then decode it [30]. Following these trends, the signal of  $V_1$  is first decoded followed by  $V_2$  and so on. Thus,  $V_1$  cannot apply SIC and decodes its signal by treating the signals of all other mobile vehicles as noise, while  $V_j$  decodes its signal after eliminating interference from all other vehicles by applying SIC technique. After the SIC process, the received signal of  $V_j$  at RSU can be expressed as:

$$y_j = g_j \sqrt{p_j} z_j + g_j \sum_{i=1}^{j-1} \sqrt{p_i} z_i + N_j, \quad (1)$$

where  $g_j$  is the channel gain between  $V_j$  and RSU in the uplink transmission,  $p_j$  represents the transmit power of  $V_j$ , and  $z_j$  is the data symbol of  $V_j$ , respectively. The second term in (1) denotes the interference of other vehicles sharing the same spectrum resource in which  $p_i$  is the transmit power and  $z_i$  is the data symbol of  $V_i$  at RSU, respectively. The noise term  $N_j \sim \mathcal{CN}(0, \sigma^2)$  is the additive white Gaussian noise with zero mean and variance  $\sigma^2$ . Based on the received signal expressed in (1), the achievable rate of  $V_j$  at RSU can be expressed as:

$$R_j = \rho_j \log_2(1 + \gamma_j), \quad (2)$$

<sup>2</sup>As per [28], [29], we sort the channel gains of different vehicles in ascending order for efficient SIC decoding at receivers.

where

$$\gamma_j = \frac{p_j |g_j|^2}{|g_j|^2 \sum_{i=1}^{j-1} \rho_i p_i + \sigma^2}, \quad (3)$$

is the SINR of  $V_j$ , and  $\rho_j$  in (2) denotes the binary variable for vehicle selection such as  $\rho_j = 1$ , if  $V_j$  is selected for communication and  $\rho_j = 0$ , otherwise.

To make the SIC process successful at RSU, the transmit power of all mobile vehicles must satisfy the minimum required gap as [31]:

$$\rho_j p_j |g_j|^2 - \sum_{i=j+1}^J \rho_i p_i |g_i|^2 \geq \beta, \quad (4)$$

where  $\beta$  is the minimum power gap between vehicles' signals to apply SIC process successfully at the RSU. Following the condition in (4), the  $J$  vehicles transmit powers must satisfy as  $p_1 > p_2 > \dots > p_j > \dots > p_J$ . It is important to note that the SIC constraints for an uplink network where  $J$  mobile vehicles are sharing the same spectrum resource will always be  $(J - 1)$  [32]. This is because when  $J$  mobile vehicles are communicated on the same spectrum resource using ascending or descending order of channel gains, a mobile vehicle having a weak channel gain can apply a SIC technique at RSU and decodes all other mobile vehicle signals first before decoding its own signal. The mobile vehicle with strong channel gain, however, can not use the SIC technique at RSU and decodes its signal by treating the other mobile vehicle's interference as noise. Thus, the SIC constraints of  $J$  mobile vehicles on the same spectrum resource are always  $J - 1$  in power-domain NOMA. Next, we discuss the joint formulation of energy and spectrum efficiency optimizations.

### B. MULTIOBJECTIVE PROBLEM FORMULATION

Our objective is to jointly maximize the sum-rate and minimize the total transmit power of uplink NOMA vehicular network while satisfying the constraints of QoS, maximum transmit power and successful SIC process. These joint objectives can be achieved by solving a multiobjective optimization problem which can be formulated as (P1):

$$\begin{aligned} \text{(P1)} \quad & \text{Max}_{\rho_j p_j} \sum_{j=1}^J \rho_j R_j \quad \text{and} \quad \text{Min}_{\rho_j p_j} \sum_{j=1}^J \rho_j p_j, \\ \text{s.t.} \quad & \text{C1: } \rho_j R_j \geq R_{min}, \quad \forall j, \\ & \text{C2: } \rho_j p_j \leq P_{max}, \quad \forall j, \\ & \text{C3: } \rho_j p_j |g_j|^2 - \sum_{i=j+1}^J \rho_i p_i |g_i|^2 \geq \beta, \quad \forall j, i, \\ & \text{C4: } \rho_j p_j \geq 0, \quad \forall j, \\ & \text{C5: } \rho_j \in \{0, 1\}, \quad \forall j. \end{aligned} \quad (5)$$

where the two objectives are for total transmit power minimization and sum-rate maximization, respectively. Constraint C1 guarantees the QoS requirement of each vehicle where  $R_{min}$  denotes the minimum achievable rate to obtain per vehicle QoS requirements. Constraint C2 limits the mobile

vehicles maximum transmit power where  $P_{max}$  represents the battery power budget of  $V_j$ . Constraint C3 ensures the successful completion of SIC process at RSU for  $V_j$ . Besides, the constraint in C4 demonstrate the non-negative transmit power of  $V_j$ . Finally, constraint C5 shows the binary variable for optimal vehicle selection such that  $\rho_j = 1$ , if  $V_j$  is selected for communication, and  $\rho_j = 0$ , otherwise.

In this optimization framework, the optimal vehicle selection before NOMA transmission should satisfy the following criterion

$$\rho_j^* = \begin{cases} 1 & \text{if } j = \operatorname{argmax}_{j \in J} R_j \\ 0 & \text{otherwise.} \end{cases} \quad (6)$$

where all the selected vehicles transmit over single-carrier according to the power-domain NOMA principle. By considering the decoding complexity of SIC at the receivers, we define a set of active vehicles at any given time as  $\mathcal{A}$ , where  $\mathcal{A}$  is a subset of set  $\mathcal{V}$  such as  $|\mathcal{A}| \ll \mathcal{V}$ . Moreover,  $\mathcal{A}$  can keep at most  $\mathcal{A}_{max}$  active vehicles at one time. In each interval, we first search an optimal  $V_j^*$  according to (6) which provides a high data rate among all vehicles. Then we record this  $V_j^*$  on  $\mathcal{A}$  and exclude it from set  $\mathcal{V}$ . Similarly, we find another vehicle that provides a high data rate after  $V_j^*$  and repeats the same process. Finally, we check the number of optimal vehicles in  $\mathcal{A}$ . If the number of vehicles is less than  $\mathcal{A}_{max}$ , continue the aforementioned procedure to select more optimal vehicles. However, the process is terminated when the number of vehicles in  $\mathcal{A}$  is equal to  $\mathcal{A}_{max}$ .

The complexity of proposed vehicle selection algorithm in terms of iterations depends on the number of vehicles in the system. If the number of vehicles in the system is  $J$ , then the complexity of the proposed vehicle selection algorithm in each iterations can be computed as  $\mathcal{O}(J^2)$ . Now let us assume that the total iterations needed for algorithm is  $T$ , then the total complexity of the proposed vehicle selection algorithm has became  $\mathcal{O}(TJ^2)$ .

### III. PROPOSED SOLUTIONS

After selecting the optimal mobile vehicles, now  $\mathcal{A}$  represents all active vehicles where  $\rho_j = 1$ . Next we discuss the performance of uplink NOMA transmission in the joint metrics of sum-rate maximization and total transmit power minimization. These can be achieved by joint optimization of optimal power allocation to the mobile vehicles in the uplink transmission. Further, a low complexity benchmark single-objective optimization scheme of sum-rate maximization is also provided.

#### A. PROPOSED MULTIOBJECTIVE SOLUTION

In multiobjective optimization, more than one objectives need to be maximized or minimized simultaneously [33]. Here, we use multiobjective optimization in which optimal decisions need to be taken as a tradeoff between two different objectives [34]. Generally, it is very hard to find a single solution for optimizing multiple objectives simultaneously.

More specifically, there is no solution exist that optimizes one objective without degrading other objectives, this state is known as Pareto optimality [35]. Pareto optimal is a set of non-dominated and weak solutions where users are able to choose its preferred optimal solution. To compute the joint optimization of power control, we apply the weighted-sum method to handle the multiobjective optimization problem [36]. This has been regarded as one of the most popular methods for solving the multiobjective optimization problem [35], [37]. By this method, the multiple objective functions can be linearly combined into a single objective function. This can be achieved through weighting coefficients which reflect the required preferences [38]. More specifically, the weighting coefficients show the tradeoff among multiple conflicting objectives. To efficiently apply this method, we reformulate the optimization problem (P1) as:

$$\begin{aligned} \text{(P2)} \quad & \text{Min } \alpha \sum_{j \in \mathcal{A}} p_j - (1 - \alpha) \sum_{j \in \mathcal{A}} R_j, \\ \text{s.t. C1: } & R_j \geq R_{min}, \quad \forall j \in \mathcal{A}, \\ \text{C2: } & p_j \leq P_{max}, \quad \forall j \in \mathcal{A}, \\ \text{C3: } & p_j |g_j|^2 - \sum_{\substack{i=j+1 \\ i \in \mathcal{A}}} p_i |g_i|^2 \geq \beta, \quad \forall j, i \in \mathcal{A}, \\ \text{C4: } & p_j \geq 0, \quad \forall j \in \mathcal{A}. \end{aligned} \quad (7)$$

where  $\alpha$  in (7) represents the weighting coefficient which lies between 0 and 1 such that  $0 \leq \alpha \leq 1$ , and shows the trade-off between two conflicting objective functions. Here, the higher values of  $\alpha$  enhance the sum-rate of mobile vehicles and lower values reduce the total transmit power of mobile vehicles, respectively. Moreover, the proper selection of  $\alpha$  depends on the model of vehicle transmission, i.e., if the rate of mobile vehicles is crucial, the higher values of  $\alpha$  are chosen. On the other side, if the power of mobile vehicles is critical, the lower values of  $\alpha$  are selected.

The multiobjective optimization problem (P2) is a convex problem (see Appendix A and proof therein). Therefore, we employ dual-decomposition methods to obtain the optimal solution [39]. The Lagrangian function of problem (P2) can be expressed as:

$$\begin{aligned} L(p_j, \lambda_j, \mu_j, \eta_j) = & \alpha \sum_{j \in \mathcal{A}} p_j - (1 - \alpha) \sum_{j=1}^J R_j \\ & + \sum_{j \in \mathcal{A}} \lambda_j (R_j - R_{min}) + \sum_{j \in \mathcal{A}} \mu_j (P_{max} - p_j) \\ & + \sum_{j \in \mathcal{A}} \eta_j \left( p_j |g_j|^2 - \sum_{\substack{i=j+1 \\ i \in \mathcal{A}}} p_i |g_i|^2 - \beta \right), \end{aligned} \quad (8)$$

where  $\lambda_j$ ,  $\mu_j$  and  $\eta_j$  are the Lagrangian multipliers also called dual variables. Using this expression, the dual problem of optimization problem (P2) can be derived as:

$$\begin{aligned} & \text{Max}_{\lambda_j, \mu_j, \eta_j} D(\lambda_j, \mu_j, \eta_j), \\ \text{subject to: } & \lambda_j, \mu_j, \eta_j. \end{aligned} \quad (9)$$

where

$$D(\lambda_j, \mu_j, \eta_j) = \min_{p_j} L(p_j, \lambda_j, \mu_j, \eta_j). \quad (10)$$

Now by applying KKT conditions as in Appendix B, the closed-form expression of  $p_j$  for  $V_j$  can be derived as:

$$p_j^* = \left[ \frac{(\alpha + \lambda_j)|g_j|^2 - \Pi_j|g_j|^2 p_i - \sigma^2(\Pi_j)}{|g_j|^2(\Pi_j)} \right]^+, \quad (11)$$

where  $(\theta)^+ = \max(0, \theta)$ , and

$$\begin{aligned} & \Pi_j \\ &= \mu_i - \sum_{\substack{i=j+1 \\ i \in \mathcal{A}}} \eta_i |g_i|^2 - \alpha + \sum_{\substack{l=i+1 \\ l \in \mathcal{A}}} \\ & \times \frac{(\alpha + \lambda_i)|g_l|^2}{\left( \sum_{f=l+1} p_f |g_f|^2 + \sigma^2 \right)^2 + \left( \sum_{f=l+1} p_f |g_f|^2 + \sigma^2 \right) p_l |g_l|^2}. \end{aligned} \quad (12)$$

With the optimal value of  $p_j^*$ , the dual problem becomes

$$\begin{aligned} & \text{Max}_{\lambda_j, \mu_j, \eta_j} \alpha \sum_{j \in \mathcal{A}} p_j^* - (1 - \alpha) \left( \sum_{j \in \mathcal{A}} R_j^* \right) \\ & + \sum_{j \in \mathcal{A}} \lambda_j (R_j^* - R_{min}) + \sum_{j \in \mathcal{A}} \mu_j (P_{max} - p_j^*) \\ & + \sum_{j \in \mathcal{A}} \eta_j \left( p_j^* |g_j|^2 - \sum_{\substack{i=j+1 \\ i \in \mathcal{A}}} p_i |g_i|^2 - \beta \right), \\ & \text{s.t. } \lambda_j, \mu_j, \eta_j. \end{aligned} \quad (13)$$

Now the dual variables in (13) can be obtained and iteratively update using sub-gradient method as [40]:

$$\begin{aligned} & \lambda_j(itr + 1) \\ &= [\lambda_j(itr) + \omega(itr) \times (R_{min} - R_j)]^+, \quad \forall j \in \mathcal{A}, \end{aligned} \quad (14)$$

$$\begin{aligned} & \mu_j(itr + 1) \\ &= [\mu_j(itr) + \omega(itr) \times (p_j - P_{max})]^+, \quad \forall j \in \mathcal{A}, \end{aligned} \quad (15)$$

$$\begin{aligned} & \eta_j(itr + 1) \\ &= \left[ \eta_j(itr) + \omega(itr) \right. \\ & \left. \times \left( \beta - \left( p_j |g_j|^2 - \sum_{\substack{i=j+1 \\ i \in \mathcal{A}}} p_i |g_i|^2 \right) \right) \right]^+, \quad \forall j, i \in \mathcal{A}. \end{aligned} \quad (16)$$

where  $itr$  is the iteration index, and  $\omega$  is the step size. In each iteration,  $\lambda_j$ ,  $\mu_j$  and  $\eta_j$  are updated using  $p_j^*$  obtained from (11). In the subsequent iterations, the optimal values of  $\lambda_j$ ,  $\mu_j$  and  $\eta_j$  are used to calculate the optimal  $p_j^*$ . The iterative process continues until convergence.

The complexity of proposed power allocation technique in terms of iterations depends on the number of selected vehicles in the system. If the number of selected vehicles in the system is  $\mathcal{A}$ , then the complexity of the proposed vehicle selection algorithm in each iterations can be computed as  $\mathcal{O}(\mathcal{A}^2)$ . It is important to note that the complexity of the proposed power allocation technique increases when the number selected

TABLE 2. Simulation parameters.

Parameter	Definition
Number of total vehicles in the network	$J = 18$
Active mobile vehicles in $\mathcal{A}$ at one time	$\mathcal{A} = 3$
Vehicle battery power	$P_{max} = 4 \text{ W}$
Channels consideration	Nakagami-m fading
Weighting coefficient	$\alpha = 0.6$ to $1$
Per vehicle QoS requirement	$R_{min} = 1 \text{ bits/sec/Hz}$
Noise power	$\sigma^2 = 0.1$
Power gap among vehicles	$\theta = 0.5 \text{ W}$
Average channel realization	$10^4$ realizations

vehicles increases. Let us consider that the maximum number of selected vehicles for NOMA transmission is  $\mathcal{A}_{max}$  and the total number of iterations needed for algorithm is  $T$ , then the total complexity of the proposed power allocation algorithm has become  $\mathcal{O}(T \mathcal{A}_{max}^2)$ .

### B. BENCHMARK SINGLE-OBJECTIVE SOLUTION

The proposed solution in Section III-A provides a multiobjective optimization for sum rate maximization and total transmit power minimization in uplink NOMA vehicular transmission. In this subsection, to reduce the computational complexity, we present a benchmark single-objective optimization scheme where only power allocation is optimized for sum-rate maximization. Without energy efficiency, the power optimization problem can be formulated as (P3):

$$\begin{aligned} & \text{(P3) Max}_{p_j} \sum_{j \in \mathcal{A}} R_j, \\ & \text{s.t. C1: } R_j \geq R_{min}, \quad \forall j \in \mathcal{A}, \\ & \text{C2: } p_j \leq P_{max}, \quad \forall j \in \mathcal{A}, \\ & \text{C3: } p_j |g_j|^2 - \sum_{\substack{i=j+1 \\ i \in \mathcal{A}}} p_i |g_i|^2 \geq \beta, \quad \forall j, i \in \mathcal{A}, \\ & \text{C4: } p_j \geq 0, \quad \forall j \in \mathcal{A}. \end{aligned} \quad (17)$$

The problem (P3) is convex and can also be solved by dual-decomposition method with similar steps as discussed in multiobjective optimization solution. However, the detailed steps are omitted here for the sake of brevity. Moreover, the complexity of the single-objective optimization scheme based on KKT conditions can be found in [4].

### IV. PERFORMANCE EVALUATION

In this section, we provide some detailed insights on the vehicular network architecture and evaluate the performance of the proposed multiobjective optimization framework. The results were obtained by performing Monte-Carlo simulations in MATLAB by taking  $10^4$  channel realizations. Throughout the results, the term ‘‘Benchmark NOMA Scheme’’ refers to the single objective scheme as detailed in Section III-B. Whereas, the term ‘‘Conventional OMA Scheme’’ denotes the proposed multiobjective framework applied to OMA. The details of the simulation parameters and their corresponding values are provided in Table 2.

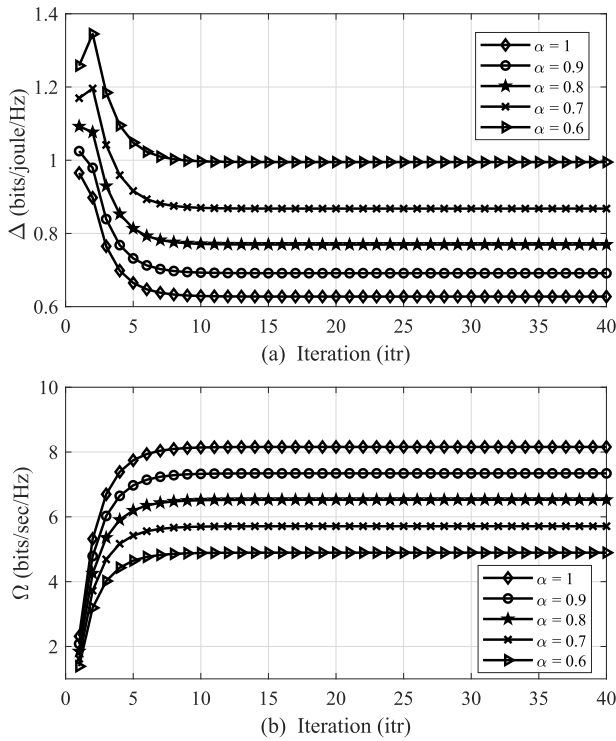


FIGURE 2. Performance of the proposed multiobjective solution with different values of  $\alpha$ ; (a) Total energy efficiency  $\Delta$ , (b) Sum-rate  $\Omega$ .

In this paper, we define the energy efficiency (bits/joule/Hz) of the proposed V2I network as the ratio of mobile vehicles sum-rate to the total transmit power consumption of mobile vehicles plus circuit power consumption. Mathematically, we denote it as  $\Delta$  in this section, and it can be formulated as:

$$\Delta = \frac{\left(\sum_{j \in \mathcal{A}} \rho_j \log_2(1 + \gamma_j)\right) \text{bits/sec/Hz}}{\left(\sum_{j \in \mathcal{A}} P_j + P_c\right) W}, \quad (18)$$

where  $p_c$  represents the circuit power consumption of mobile vehicles. Accordingly, the sum-rate (represented as  $\Omega$ ) of V2I network can be defined as:

$$\Omega = \left(\sum_{j \in \mathcal{A}} \rho_j \log_2(1 + \gamma_j)\right) \text{bits/sec/Hz}. \quad (19)$$

Fig. 2 (a) shows the convergence of the energy efficiency ( $\Delta$ ) against the number of iterations (*itr*). Note that for an increase in the values of  $\alpha$ , the  $\Delta$  declines. Whereas for smaller values of  $\alpha$  the  $\Delta$  improves. In particular, when  $\alpha = 1$ , the  $\Delta$  is 0.65 bits/joule/Hz which increases to 1 bits/joule/Hz when  $\alpha = 0.6$ . By contrast, Fig. 2 (b) indicates that a decrease in the value  $\alpha$  reduces the overall sum-rate ( $\Omega$ ). More specifically, as  $\alpha$  varies from 1 to 0.6, the corresponding values of the  $\Omega$  reduce from 8.2 bits/sec/Hz to just 4.5 bits/sec/Hz. However, regardless of the value of  $\alpha$ , one can note that the proposed multiobjective optimization framework converges within a reasonable number of *itr*.

In Fig. 3, we have demonstrated the  $\Delta$  as a function of increasing transmit power. We have compared the proposed

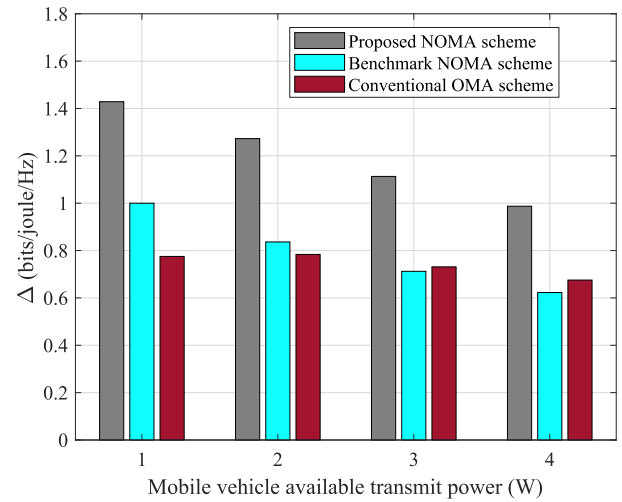


FIGURE 3. Available transmit power of mobile vehicle versus  $\Delta$  for  $\alpha = 0.6$ ,  $R_{min} = 1$  bits/sec/Hz.

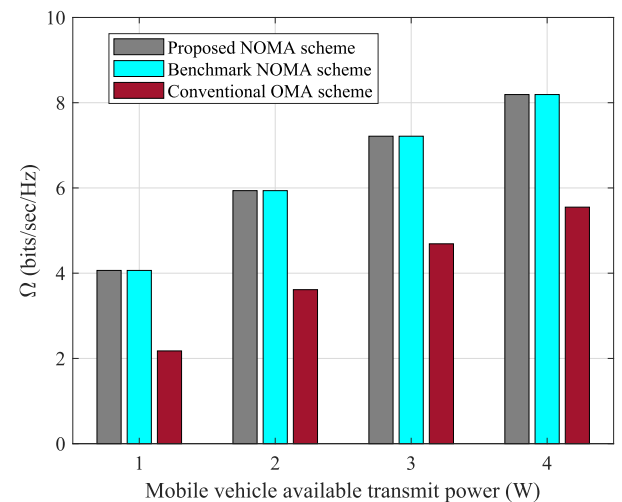


FIGURE 4. Sum rate  $\Omega$  versus mobile vehicle available battery power (W) for  $\alpha = 1$ ,  $R_{min} = 1$  bits/sec/Hz.

optimization scheme with the single objective benchmark NOMA scheme and the conventional OMA scheme. In general, we can observe that the  $\Delta$  decreases with an increase in the transmit power of the vehicle. However, the proposed NOMA scheme continues to outperform both benchmark NOMA and conventional OMA schemes. Also, it can be observed that at higher values of transmit power (i.e., 4 W), the conventional OMA scheme outperforms the benchmark NOMA scheme. This shows the applicability of our proposed multiobjective framework for not only NOMA but OMA as well. In a similar manner, Fig. 4 shows the  $\Omega$  for the three schemes. Again, for a particular value of  $\alpha$ , the proposed approach seems to perform close to the benchmark NOMA scheme. Whereas, it clearly outperforms the conventional OMA scheme, especially at the larger values of the transmit power.

To further elaborate on the significance of  $\alpha$ , Fig. 5 goes on to illustrate the impact of different values of  $\alpha$  on  $\Delta$  and  $\Omega$ . It can be seen from Fig. 5 (a) that an increase in the value

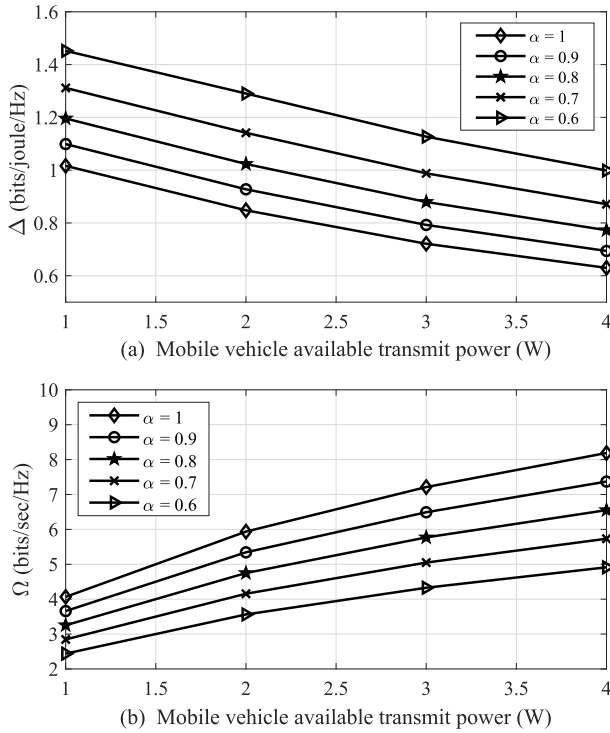


FIGURE 5. Performance of the proposed multiobjective solution with different values of  $\alpha$ ; (a) Total energy efficiency  $\Delta$ , (b) Sum-rate  $\Omega$ .

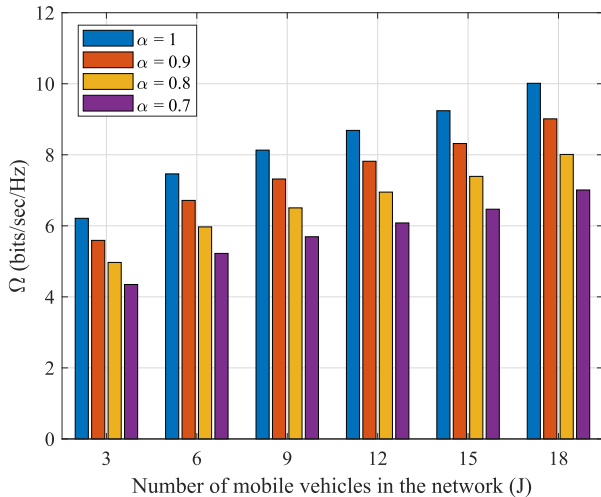


FIGURE 6. The number of vehicles  $J$  in the network versus the  $\Omega$  of the proposed NOMA scheme for different values of  $\alpha$  when  $P_{max} = 4$  W,  $R_{min} = 1$  bits/sec/Hz.

of  $\alpha$  causes a reduction in  $\Delta$ . Moreover, as the values of  $\alpha$  decrease, the gap between different curves grow to show the impact of  $\alpha$  at larger values of transmit power. On the other hand, Fig. 5 (b) shows the impact of  $\alpha$  against increasing values of transmit power. In contrast, we can observe that the  $\Omega$  improves with larger values of transmit power from the vehicle. Furthermore, it can also be observed that the increasing values of  $\alpha$  favor the  $\Omega$ , resulting in significant improvement when  $\alpha = 1$ .

The impact of the increasing number of vehicles on the performance of the network is demonstrated in Fig. 6. In general,

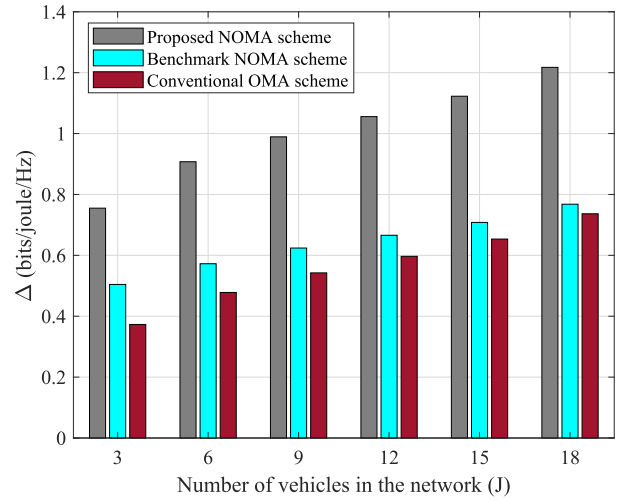


FIGURE 7. The number of mobile vehicles  $J$  in the network versus  $\Delta$  when  $\alpha = 0.6$ ,  $P_{max} = 4$  W,  $R_{min} = 1$  bits/sec/Hz.

we note an increase in the  $\Omega$  when the number of vehicles in the network grows. This improvement can be attributed to the improvement in diversity gains ensure by (6). As a result of a decrease in value of  $\alpha$  does not influence the performance of the vehicular network much when the number of vehicles is large. Similar trends can be observed in Fig. 7, where the  $\Delta$  is plotted by keeping the value of  $\alpha$  fixed at 0.6. As one can note, the proposed optimization scheme continues to outperform the benchmark NOMA scheme and conventional OMA scheme. Again, this improvement is because of improved diversity gains due to the larger number of vehicles in the network.

Fig. 8 shows the impact of the Nakagami- $m$  factor for both  $\Delta$  and  $\Omega$ . We can observe from Fig. 8 (a) that an increase in the value of the Nakagami- $m$  factor results in improving the  $\Delta$  of the network. In this regard, it is worth highlighting that when  $m = 1$ , the channel characteristics become similar to a Rayleigh fading channel. Similar trends can be observed in Fig. 8 (b), where an improvement in channel conditions result in considerable performance gains in terms of  $\Omega$ .

## V. CONCLUSION AND FUTURE WORK

V2I communication is an integral part of the vehicular networks. By integrating efficient NOMA techniques in V2I communication, the performance of such a network can be significantly improved. In this backdrop, this work has provided a multiobjective optimization framework to improve the sum-rate and energy efficiency of the NOMA-enabled V2I communications. The proposed framework is not only more energy efficient but also has the capability to improve the overall sum-rate of the network. As illustrated by extensive simulations, the proposed framework can outperform the conventional single-objective NOMA and traditional OMA approaches by a great margin. Moreover, it was shown that an increase in the uplink transmitting vehicles can indeed improve the performance of the network, when operating under the proposed optimization framework, due to the



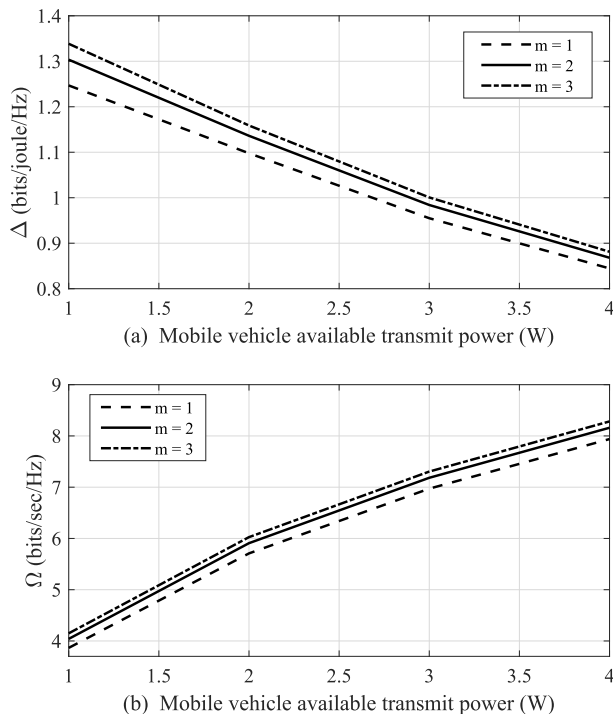


FIGURE 8. Performance of the proposed multiobjective solution with different values of  $m$ ; (a)  $\Delta$ , (b)  $\Omega$ .

increased diversity gains. Finally, the performance of the network under different channel conditions was also illustrated. The results provided in this work are expected to lay the foundations for an extensive number of future studies in this domain.

The results provided in our work are self-sufficient, however, they are by no means conclusive and can be extended in a number of ways. For instance, future studies can consider a more dynamic network setup by introducing the concept of vehicle association. In this way, the performance of our proposed scheme can be evaluated and a more extended version can be proposed that takes into account the vehicle association aspects. Another promising direction can be to evaluate the proposed multiobjective optimization framework for cooperative vehicular networks. The cooperation among vehicles is expected to improve the performance of these networks. Moreover, the proposed optimization framework could be extended to different types of cooperation schemes. These exciting extensions of the proposed optimization framework would be performed in future work.

APPENDIXES

APPENDIX A

CONCAVITY/CONVEXITY PROOF OF (P2)

Here we show the convexity/concavity proof of the proposed optimization problem (P2). A function can be concave/convex if its Hessian matrix is negative definite. It is worth noting that a Hessian matrix will be negative definite if its leading principal minors are alternate in sign, i.e., negative for odd and positive for even numbers. Next, we derive the Hessian matrix and then prove it as a negative definite.

Firstly, we derive the objective function of proposed joint optimization problem (P2) as:

$$\text{Min } \beta \sum_{j \in \mathcal{A}} p_j - (1 - \alpha) \sum_{j \in \mathcal{A}} R_j, \quad (20)$$

where in (20), one can be observed that the first segment is a linear function of power. The rate function in second segment is strictly concave-convex function.

Let us assume the active mobile vehicles per time slot are three, i.e.,  $\mathcal{A} = 3$ . Accordingly, the channel powers of these mobile vehicles are sorted as  $|g_1|^2 \leq |g_2|^2 \leq |g_3|^2$ . Then, the sum rate can be derived as:

$$R_{\text{sum}} = \log_2(1 + \gamma_1) + \log_2(1 + \gamma_2) + \log_2(1 + \gamma_3), \quad (21)$$

By expanding the rate terms of vehicles, we have

$$R_{\text{sum}} = \log_2 \left( 1 + \frac{p_3 |h_3|^2}{\sigma^2} \right) + \log_2 \left( 1 + \frac{p_2 |h_2|^2}{p_3 |h_2|^2 + \sigma^2} \right) + \log_2 \left( 1 + \frac{p_1 |h_1|^2}{(p_2 + p_3) |h_1|^2 + \sigma^2} \right), \quad (22)$$

Next we define the Hessian matrix of (22) as:

$$H = \begin{bmatrix} \left( \frac{\partial R_{\text{sum}}}{\partial p_1} \right) & \left( \frac{\partial R_{\text{sum}}}{\partial p_1 \partial p_2} \right) & \left( \frac{\partial R_{\text{sum}}}{\partial p_1 \partial p_3} \right) \\ \left( \frac{\partial R_{\text{sum}}}{\partial p_2} \right) & \left( \frac{\partial R_{\text{sum}}}{\partial p_2} \right) & \left( \frac{\partial R_{\text{sum}}}{\partial p_2} \right) \\ \left( \frac{\partial R_{\text{sum}}}{\partial p_3} \right) & \left( \frac{\partial R_{\text{sum}}}{\partial p_3} \right) & \left( \frac{\partial R_{\text{sum}}}{\partial p_3} \right) \end{bmatrix} \quad (23)$$

By calculating the partial derivations, we get

$$H = \begin{bmatrix} -\xi & -\xi & -\xi \\ -\xi & -\xi + \xi' - \varrho & -\xi + \xi' - \varrho \\ -\xi & -\xi + \xi' - \varrho & -\xi + \xi' - \varrho + \varrho' - \vartheta \end{bmatrix} \quad (24)$$

where

$$\xi = \left( \frac{|g_3|^2}{(p_1 + p_2 + p_3) |g_3|^2 + \sigma^2} \right)^2, \quad (25)$$

$$\xi' = \left( \frac{|g_3|^2}{(p_2 + p_3) |g_3|^2 + \sigma^2} \right)^2, \quad (26)$$

$$\varrho = \left( \frac{|g_2|^2}{(p_2 + p_3) |g_2|^2 + \sigma^2} \right)^2, \quad (27)$$

$$\varrho' = \left( \frac{|g_2|^2}{p_3 |g_2|^2 + \sigma^2} \right)^2, \quad (28)$$

$$\vartheta = \left( \frac{|g_1|^2}{p_3 |g_2|^2 + \sigma^2} \right)^2. \quad (29)$$

Now the first order principle in (24) can be formulated as

$$\det |H_1| = -\xi. \quad (30)$$

Accordingly, the second order principle minor can be stated as:

$$\begin{aligned} \det |H_2| &= \xi(\varrho - \xi') \\ &= \xi \left( \left( \frac{|g_2|^2}{p_2 |g_2|^2 + \sigma^2} \right)^2 - \left( \frac{|g_3|^2}{p_2 |g_3|^2 + \sigma^2} \right)^2 \right) \end{aligned} \quad (31)$$

where after taking least common multiple (LCM), we can obtain as:

$$= \xi \left( \frac{(2p_2 |g_3|^2 |g_2|^2 + |g_3|^2 + |g_2|^2)(|g_2|^2 - |g_3|^2)}{(p_2 |g_3|^2 + \sigma^2)^2 (p_2 |g_2|^2 + \sigma^2)} \right). \quad (32)$$

Finally, the third principle minor can be expressed as:

$$\begin{aligned} \det |H_3| &= -\xi(\varrho - \xi')(\vartheta - \varrho') \\ &= -\xi \left( \left( \frac{|g_2|^2}{p_2|g_2|^2 + \sigma^2} \right)^2 - \left( \frac{|g_3|^2}{p_2|g_3|^2 + \sigma^2} \right)^2 \right) \\ &\quad \times \left( \left( \frac{|g_1|^2}{p_3|g_2|^2 + \sigma^2} \right)^2 - \left( \frac{|g_2|^2}{p_3|g_2|^2 + \sigma^2} \right)^2 \right), \end{aligned} \quad (33)$$

Again, by taking LCM of (33), it can be written as:

$$\begin{aligned} &= -\xi \\ &\quad \times \left( \frac{(2(p_2 + p_3)|g_3|^2|g_2|^2 + |g_3|^2 + |g_2|^2)(|g_2|^2 - |g_3|^2)}{((p_2 + p_3)|g_3|^2 + \sigma^2)((p_2 + p_3)|g_2|^2 + \sigma^2)} \right) \\ &\quad \times \left( \frac{(2p_3|g_2|^2|g_1|^2 + |g_2|^2 + |g_1|^2)(|g_1|^2 - |g_2|^2)}{(p_3|g_2|^2 + \sigma^2)(p_3|g_1|^2 + \sigma^2)} \right). \end{aligned} \quad (34)$$

where  $\xi, \xi', \varrho, \varrho'$  and  $\vartheta$  in (34) are all positive. Therefore, the first and second order principle minors are negative and the third one is positive. Thus, the proposed optimization problem (P2) is concave-convex function.

### APPENDIX B CLOSED-FORM EXPRESSION DERIVATIONS

To perform the SIC process successfully at receivers, we have sorted the channel gain of three vehicles as  $|g_1|^2 \leq |g_2|^2 \leq |g_3|^2$ . Accordingly, when  $j = 3$ , it shows the vehicle with strongest channel gain (i.e.,  $V_3$ ), and can not apply SIC. Thus, it decodes the signal with the interference from all other vehicles with lower channel gains. Note that these interference of other vehicles are acted as a noise for  $V_3$ . Therefore, the closed-form expression of  $V_3$  can be calculated as:

$$L(p_3, \lambda_3, \mu_3) = \alpha p_3 - (1 - \alpha)R_3 + \lambda_3(R_3 - R_{min}) + \mu_3(P_{max} - p_3), \quad (35)$$

By taking  $\frac{\partial L(p_3, \lambda_3, \mu_3)}{\partial p_3}$ , it can be written as:

$$\frac{\partial L(p_3, \lambda_3, \mu_3)}{\partial p_3} = \alpha p_3 + ((\alpha - 1) + \lambda_3)R_3 - \mu_3 p_3, \quad (36)$$

Expanding the rate term of  $V_3$ , we have

$$\begin{aligned} &\frac{\partial L(p_3, \lambda_3, \mu_3)}{\partial p_3} \\ &= \alpha p_3 + ((\alpha - 1) + \lambda_3) \\ &\quad \times \log_2 \left( 1 + \frac{p_3|g_3|^2}{\sum_{i=1}^2 p_i|g_3|^2 + \sigma^2} \right) - \mu_3 p_3, \end{aligned} \quad (37)$$

After straightforward derivations, it can be given as:

$$\begin{aligned} &\frac{\partial L(p_3, \lambda_3, \mu_3)}{\partial p_3} = \alpha + ((\alpha - 1) + \lambda_3) \\ &\quad \times \left( \frac{|g_3|^2}{\sum_{i=1}^2 p_i|g_3|^2 + p_3|g_3|^2 + \sigma^2} \right) - \mu_3, \end{aligned} \quad (38)$$

Solving for  $p_3^*$ , we set  $\frac{\partial L(p_3, \lambda_3, \mu_3)}{\partial p_3} = 0$  as:

$$\begin{aligned} &\alpha + ((\alpha - 1) + \lambda_3) \\ &\quad \times \left( \frac{|g_3|^2}{\sum_{i=1}^2 p_i|g_3|^2 + p_3|g_3|^2 + \sigma^2} \right) - \mu_3 = 0, \end{aligned} \quad (39)$$

By simplification, it can be formulated as:

$$\frac{\alpha + ((\alpha - 1) + \lambda_3)|g_3|^2}{\mu_3 - \alpha} - (p_1 + p_2)|g_3|^2 - \sigma^2 = p_3|g_3|^2, \quad (40)$$

Thus, the optimal power of  $V_3$  can be derived as:

$$p_3^* = \left[ \frac{((\alpha - 1) + \lambda_3)|g_3|^2 - \zeta_3((p_1 + p_2)|g_3|^2 - \sigma^2)}{\zeta_3|g_3|^2} \right]^+. \quad (41)$$

where  $\zeta_3 = \mu_3 - \alpha$ .

For second vehicle when  $j = 2$ ,  $V_2$  can apply SIC, first decodes and subtract the signal  $V_3$ , and then decode its own signal. Note that  $V_2$  can not decode  $V_1$  signal. Thus, the closed-form expression of  $V_2$  can be stated as:

$$\begin{aligned} L(p_2, \lambda_2, \mu_2) &= \alpha p_2 - (1 - \alpha)R_2 + \lambda_2(R_2 - R_{min}) \\ &\quad + \mu_2(P_{max} - p_2) + \eta_2(p_2|g_2|^2 - p_3|g_3|^2 - \beta), \end{aligned} \quad (42)$$

By taking  $\frac{\partial L(p_2, \lambda_2, \mu_2)}{\partial p_2}$  and cancel the constant terms, we obtain as:

$$\begin{aligned} &\frac{\partial L(p_2, \lambda_2, \mu_2)}{\partial p_2} = \alpha p_2 + ((\alpha - 1) + \lambda_2)R_2 \\ &\quad - \mu_2 p_2 + \eta_2(p_2|g_2|^2), \end{aligned} \quad (43)$$

Expanding the rate term  $R_2$  of  $V_2$ , we have

$$\begin{aligned} &\frac{\partial L(p_2, \lambda_2, \mu_2)}{\partial p_2} \\ &= \alpha p_2 + ((\alpha - 1) + \lambda_2) \\ &\quad \times \log_2 \left( 1 + \frac{p_2|g_2|^2}{p_3|g_2|^2 + \sigma^2} \right) + ((\alpha - 1) + \lambda_1) \\ &\quad \times \log_2 \left( 1 + \frac{p_1|g_1|^2}{\sum_{i=2}^3 p_i|g_1|^2 + \sigma^2} \right) - \mu_2 p_2 + \eta_2(p_2|g_2|^2), \end{aligned} \quad (44)$$

After derivations, it can be computed as:

$$\begin{aligned} &\frac{\partial L(p_2, \lambda_2, \mu_2)}{\partial p_2} \\ &= \alpha + \eta_2|g_2|^2 + ((\alpha - 1) + \lambda_2) \\ &\quad \times \left( \frac{|g_2|^2}{p_3|g_2|^2 + p_2|g_2|^2 + \sigma^2} \right) - \mu_2 + ((\alpha - 1) + \lambda_1) \\ &\quad \times \left( \frac{-|g_1|^2}{(\sum_{i=2}^3 p_i|g_1|^2 + \sigma^2)^2 + (\sum_{i=2}^3 p_i|g_1|^2 + \sigma^2)p_1|g_1|^2} \right), \end{aligned} \quad (45)$$

Solving for  $p_2^*$ , we set  $\frac{\partial L(p_2, \lambda_2, \mu_2)}{\partial p_2} = 0$  as:

$$\begin{aligned} 0 &= \alpha + \eta_2|g_2|^2 + ((\alpha - 1) + \lambda_2) \\ &\quad \times \left( \frac{|g_2|^2}{p_3|g_2|^2 + p_2|g_2|^2 + \sigma^2} \right) - \mu_2 + ((\alpha - 1) + \lambda_1) \\ &\quad \times \left( \frac{-|g_1|^2}{(\sum_{i=2}^3 p_i|g_1|^2 + \sigma^2)^2 + \sum_{i=2}^3 p_i|g_1|^2 + \sigma^2 p_1|g_1|^2} \right), \end{aligned} \quad (46)$$

By simplification, it can be given as:

$$((\alpha - 1) + \lambda_2)|g_2|^2 = (p_3|g_2|^2 + p_2|g_2|^2 + \sigma^2) \times \zeta_2, \quad (47)$$

where

$$\zeta_2 = \frac{((\alpha - 1) + \lambda_1)|g_1|^2}{(\sum_{i=2}^3 p_i |g_1|^2 + \sigma^2)^2 + (\sum_{i=2}^3 p_i |g_1|^2 + \sigma^2)p_1 |g_1|^2 + \mu_2 - \eta_2 |g_2|^2 - \alpha}, \quad (48)$$

Then, the optimal power of  $V_2$  can be obtained as:

$$p_2^* = \left[ \frac{((\alpha - 1) + \lambda_2)|g_2|^2 - \zeta_2(\sigma^2 + p_3|g_2|^2)}{\zeta_2|g_2|^2} \right]^+, \quad (49)$$

Thus, in general, the optimal power of  $V_j$  can be derived as (11).

## REFERENCES

- [1] F. Jameel, Z. Chang, J. Huang, and T. Ristaniemi, "Internet of autonomous vehicles: Architecture, features, and socio-technological challenges," *IEEE Wireless Commun.*, vol. 26, no. 4, pp. 21–29, Aug. 2019.
- [2] R. Molina-Masegosa and J. Gozalvez, "LTE-V for sidelink 5G V2X vehicular communications: A new 5G technology for short-range Vehicle-to-Everything communications," *IEEE Veh. Technol. Mag.*, vol. 12, no. 4, pp. 30–39, Dec. 2017.
- [3] F. Jameel, M. A. Javed, and D. T. Ngo, "Performance analysis of cooperative V2V and V2I communications under correlated fading," *IEEE Trans. Intell. Transp. Syst.*, early access, Jul. 30, 2019, doi: 10.1109/TITS.2019.2929825.
- [4] W. U. Khan, Z. Yu, S. Yu, G. A. S. Sidhu, and J. Liu, "Efficient power allocation in downlink multi-cell multi-user NOMA networks," *IET Commun.*, vol. 13, no. 4, pp. 396–402, Mar. 2019.
- [5] X. Li, J. Li, Y. Liu, Z. Ding, and A. Nallanathan, "Residual transceiver hardware impairments on cooperative NOMA networks," *IEEE Trans. Wireless Commun.*, vol. 19, no. 1, pp. 680–695, Jan. 2020.
- [6] Z. Ali, Y. Rao, W. U. Khan, and G. A. S. Sidhu, "Joint user pairing, channel assignment and power allocation in NOMA based CR systems," *Appl. Sci.*, vol. 9, no. 20, p. 4282, 2019.
- [7] A. Ali, A. Baig, G. M. Awan, W. U. Khan, Z. Ali, and G. A. S. Sidhu, "Efficient resource management for sum capacity maximization in 5G NOMA systems," *Appl. Syst. Innov.*, vol. 2, no. 3, p. 27, 2019.
- [8] B. Di, L. Song, Y. Li, and G. Y. Li, "NOMA-based low-latency and high-reliable broadcast communications for 5G V2X services," in *Proc. GLOBECOM - IEEE Global Commun. Conf.*, Dec. 2017, pp. 1–6.
- [9] B. Di, L. Song, Y. Li, and G. Y. Li, "Non-orthogonal multiple access for high-reliable and low-latency V2X communications in 5G systems," *IEEE J. Sel. Areas Commun.*, vol. 35, no. 10, pp. 2383–2397, Oct. 2017.
- [10] H. Xiao, Y. Chen, S. Ouyang, and A. T. Chronopoulos, "Power control for clustering car-following V2X communication system with non-orthogonal multiple access," *IEEE Access*, vol. 7, pp. 68160–68171, 2019.
- [11] B. Wang, R. Zhang, C. Chen, X. Cheng, L. Yang, and Y. Jin, "Interference hypergraph-based 3D matching resource allocation protocol for NOMA-V2X networks," *IEEE Access*, vol. 7, pp. 90789–90800, 2019.
- [12] A. Anwar, B.-C. Seet, and X. Jun Li, "NOMA for V2X under similar channel conditions," *AIMS Electron. Electr. Eng.*, vol. 2, no. 1, pp. 48–58, 2018.
- [13] B. Wang, R. Zhang, C. Chen, X. Cheng, and L. Yang, "Interference hypergraph-based resource allocation (IHG-RA) for NOMA-integrated V2X networks," in *Proc. IEEE Global Commun. Conf. (GLOBECOM)*, Dec. 2018, pp. 1–6.
- [14] C. Chen, B. Wang, and R. Zhang, "Interference hypergraph-based resource allocation (IHG-RA) for NOMA-integrated V2X networks," *IEEE Internet Things J.*, vol. 6, no. 1, pp. 161–170, Feb. 2019.
- [15] S. Guo and X. Zhou, "Robust power allocation for NOMA in heterogeneous vehicular communications with imperfect channel estimation," in *Proc. IEEE 28th Annu. Int. Symp. Pers., Indoor, Mobile Radio Commun. (PIMRC)*, Oct. 2017, pp. 1–5.
- [16] S. Guo and X. Zhou, "Robust resource allocation with imperfect channel estimation in NOMA-based heterogeneous vehicular networks," *IEEE Trans. Commun.*, vol. 67, no. 3, pp. 2321–2332, Mar. 2019.
- [17] B. Fairouz, H. Abdelkrim, B. Mohamed, B. Sarah, and D. Sonia, "Uplink V2I communication based on non orthogonal multiple access," in *Proc. Int. Conf. Appl. Smart Syst. (ICASS)*, Nov. 2018, pp. 1–5.
- [18] L. P. Qian, Y. Wu, H. Zhou, and X. Shen, "Dynamic cell association for non-orthogonal multiple-access V2S networks," *IEEE J. Sel. Areas Commun.*, vol. 35, no. 10, pp. 2342–2356, Oct. 2017.
- [19] Y. Xu and X. Gu, "Resource allocation for NOMA-based V2V system," in *Proc. Int. Conf. Netw. Infrastruct. Digit. Content (IC-NIDC)*, Aug. 2018, pp. 239–243.
- [20] Y. Chen, L. Wang, Y. Ai, B. Jiao, and L. Hanzo, "Performance analysis of NOMA-SM in Vehicle-to-Vehicle massive MIMO channels," *IEEE J. Sel. Areas Commun.*, vol. 35, no. 12, pp. 2653–2666, Dec. 2017.
- [21] Z. Wang, J. Hu, G. Liu, and Z. Ma, "Optimal power allocations for relay-assisted NOMA-based 5G V2X broadcast/multicast communications," in *Proc. IEEE/CIC Int. Conf. Commun. China (ICCC)*, Aug. 2018, pp. 688–693.
- [22] H. Zheng, H. Li, S. Hou, and Z. Song, "Joint resource allocation with weighted max-min fairness for NOMA-enabled V2X communications," *IEEE Access*, vol. 6, pp. 65449–65462, 2018.
- [23] D. Zhang, Y. Liu, L. Dai, A. K. Bashir, A. Nallanathan, and B. Shim, "Performance analysis of FD-NOMA-Based decentralized V2X systems," *IEEE Trans. Commun.*, vol. 67, no. 7, pp. 5024–5036, Jul. 2019.
- [24] E. Bedeer, O. A. Dobre, M. H. Ahmed, and K. E. Baddour, "A multiobjective optimization approach for optimal link adaptation of OFDM-based cognitive radio systems with imperfect spectrum sensing," *IEEE Trans. Wireless Commun.*, vol. 13, no. 4, pp. 2339–2351, Apr. 2014.
- [25] Y. Liu, H. Zhang, K. Long, A. Nallanathan, and V. C. M. Leung, "Energy-efficient subchannel matching and power allocation in NOMA autonomous driving vehicular networks," *IEEE Wireless Commun.*, vol. 26, no. 4, pp. 88–93, Aug. 2019.
- [26] W. Xie, J. Liao, C. Yu, P. Zhu, and X. Liu, "Physical layer security performance analysis of the FD-based NOMA-VC system," *IEEE Access*, vol. 7, pp. 115568–115573, 2019.
- [27] X. Li, M. Zhao, C. Zhang, W. U. Khan, J. Wu, K. M. Rabie, and R. Kharel, "Security analysis of multi-antenna NOMA networks under I/Q imbalance," *Electronics*, vol. 8, no. 11, p. 1327, 2019.
- [28] A. Zakeri, M. Moltafet, and N. Mokari, "Joint radio resource allocation and SIC ordering in NOMA-based networks using submodularity and matching theory," *IEEE Trans. Veh. Technol.*, vol. 68, no. 10, pp. 9761–9773, Oct. 2019.
- [29] L. P. Qian, A. Feng, Y. Huang, Y. Wu, B. Ji, and Z. Shi, "Optimal SIC ordering and computation resource allocation in MEC-aware NOMA NB-IoT networks," *IEEE Internet Things J.*, vol. 6, no. 2, pp. 2806–2816, Apr. 2019.
- [30] W. U. Khan, F. Jameel, T. Ristaniemi, B. M. Elhalawany, and J. Liu, "Efficient power allocation for multi-cell uplink NOMA network," in *Proc. IEEE 89th Veh. Technol. Conf. (VTC-Spring)*, Apr. 2019, pp. 1–5.
- [31] W. U. Khan, F. Jameel, T. Ristaniemi, S. Khan, G. A. S. Sidhu, and J. Liu, "Joint spectral and energy efficiency optimization for downlink NOMA networks," *IEEE Trans. Cognit. Commun. Netw.*, early access, Oct. 7, 2019, doi: 10.1109/TCCN.2019.2945802.
- [32] M. S. Ali, E. Hossain, A. Al-Dweik, and D. I. Kim, "Downlink power allocation for CoMP-NOMA in multi-cell networks," *IEEE Trans. Commun.*, vol. 66, no. 9, pp. 3982–3998, Sep. 2018.
- [33] N. Gunantara, "A review of multi-objective optimization: Methods and its applications," *Cogent Eng.*, vol. 5, no. 1, 2018, Art. no. 1502242.
- [34] M. Naeem, A. S. Khwaja, A. Anpalagan, and M. Jaseemuddin, "Green cooperative cognitive radio: A multiobjective optimization paradigm," *IEEE Syst. J.*, vol. 10, no. 1, pp. 240–250, Mar. 2016.
- [35] K. Miettinen, *Nonlinear Multiobjective Optimization*, vol. 12. New York, NY, USA: Springer, 2012.
- [36] R. T. Marler and J. S. Arora, "The weighted sum method for multi-objective optimization: New insights," *Structural Multidisciplinary Optim.*, vol. 41, no. 6, pp. 853–862, Jun. 2010.
- [37] R. T. Marler and J. S. Arora, "Survey of multi-objective optimization methods for engineering," *Structural Multidisciplinary Optim.*, vol. 26, no. 6, pp. 369–395, Apr. 2004.
- [38] M. Robat Mili, K. A. Hamdi, F. Marvasti, and M. Bennis, "Joint optimization for optimal power allocation in OFDMA femtocell networks," *IEEE Commun. Lett.*, vol. 20, no. 1, pp. 133–136, Jan. 2016.
- [39] T. Jabeen, Z. Ali, W. U. Khan, F. Jameel, I. Khan, G. A. S. Sidhu, and B. J. Choi, "Joint power allocation and link selection for multi-carrier buffer aided relay network," *Electronics*, vol. 8, no. 6, p. 686, 2019.

- [40] W. U. Khan, "Maximizing physical layer security in relay-assisted multicarrier nonorthogonal multiple access transmission," *Internet Technol. Lett.*, vol. 2, no. 2, p. e76, Mar. 2019.



**WALI ULLAH KHAN** (Student Member, IEEE) received the B.S. degree (Hons.) in telecommunication from the University of Science and Technology Bannu, Khyber Pakhtunkhwa, Pakistan, in 2014, and the master's degree in electrical engineering from the Islamabad Campus of COMSATS Institute of Information Technology (currently known COMSATS University), Pakistan, in 2017. He is currently with the School of Information Science and Engineering, Shandong University, Qingdao, China. His research interests include convex/non-convex optimization, non-orthogonal multiple access, energy/spectral efficiency, physical layer security, heterogeneous networks, vehicular networks, machine/deep learning, and backscatter communications. He is also an Active Reviewer of several SCI journals, such as the IEEE WIRELESS COMMUNICATIONS, *EURASIP Journal on Wireless Communications and Networking*, IEEE ACCESS, the IEEE OPEN JOURNAL OF VEHICULAR TECHNOLOGY, the IEEE TRANSACTIONS ON INDUSTRIAL INFORMATICS, the *Internet Technology Letters*, and *Physical Communication*.



**FURQAN JAMEEL** received the B.S. degree in electrical engineering (under ICT R&D funded Program) from the Lahore Campus of COMSATS Institute of Information Technology (CIIT), Pakistan, in 2013, and the master's degree in electrical engineering (funded by prestigious Higher Education Commission Scholarship) from the Islamabad Campus of CIIT, in 2017. In September 2018, he visited the Simula Research Laboratory and the University of Oslo, Norway. From 2018 to 2019, he was with the University of Jyväskylä, Finland, and Nokia Bell Labs, Espoo, Finland, where he worked as a Researcher and a Summer Trainee, respectively. He is currently with the Department of Communications and Networking, Aalto University, Espoo. His research interests include modeling and performance enhancement of vehicular networks, machine/deep learning, ambient backscatter communications, and wireless power transfer. He was a recipient of the Outstanding Reviewer Award 2017 from Elsevier.



**GUFTAAR AHMAD SARDAR SIDHU** received the B.Sc. degree in computer engineering from the COMSATS Institute of Information Technology, Islamabad, Pakistan, in 2006, and the M.Sc. and Ph.D. degrees in electrical engineering from Jacobs University, Bremen, Germany, in 2009 and 2012, respectively. He is currently an Assistant Professor with the Department of Electrical and Computer Engineering, COMSATS University Islamabad. He has published more than 50 research articles in international journals and peer-reviewed conferences. His research interests include cooperative wireless communication, cognitive radio networks, multiuser multicarrier systems, heterogeneous networks, physical-layer security, energy harvesting, non-orthogonal multiple access schemes, energy management in smart grids, and economic dispatch in future renewable integrated power systems. He received the Best Paper Award at the IEEE International Wireless Communication and Signal Processing Conference, in 2010.



**MANZOOR AHMED** received the B.E. and M.S. degrees in electrical engineering and computer science from Balochistan Engineering University, Khuzdar, Pakistan, in 1996 and 2010, respectively, and the Ph.D. degree in communication and information systems from the Beijing University of Posts and Telecommunications, China, in 2015. From 1997 to 2000, he was a Lecturer with Balochistan Engineering University and a Telecomm Engineer in Government-Owned Telecommunication Service Provider NTC, Pakistan, from 2000 to 2011. He was a Postdoctoral Researcher with the Electrical Engineering Department, Tsinghua University, China, from 2015 to 2018. He is currently a Faculty Member with the Department of Computer Science and Technology, Qingdao University. His research interests include resource allocation and offloading in vehicular communications and networking, fog and edge computing, socially aware D2D communication, non-orthogonal multiple access, and physical layer security. He has several research publications in the IEEE top journals and conferences. He received several awards, including the Distinction Award from the President of Pakistan, the Best Employee Award from NTC, and the Best Paper Award from the 2014 GameNets Conference.



**XINGWANG LI** (Senior Member, IEEE) received the B.Sc. degree from Henan Polytechnic University, in 2007, the M.Sc. degree from the University of Electronic Science and Technology of China, in 2010, and the Ph.D. degree from the Beijing University of Posts and Telecommunications, in 2015. From 2010 to 2012, he was working with Comba Telecom Ltd., Guangzhou, China, as an Engineer. From 2017 to 2018, he was a Visiting Scholar with Queen's University Belfast, Belfast, U.K. He is currently an Associate Professor with the School of Physics and Electronic Information Engineering, Henan Polytechnic University, Jiaozuo, China. His research interests include MIMO communication, cooperative communication, hardware constrained communication, non-orthogonal multiple access, physical layer security, unmanned aerial vehicles, and the Internet-of-Things. He is currently an Editor on the Editorial Board of IEEE ACCESS, *Computer Communications*, *Physical Communication*, and the *KSII Transactions on Internet and Information Systems*. He is also a Lead Guest Editor of the special issue on Recent Advances in Physical Layer Technologies for 5GEnabled Internet of Things of Wireless Communications and Mobile Computing. He has served as the many TPC/Co-Chair, such as the IEEE Global Communications Conference (GLOBECOM), the IEEE International Conference on Communications in China (CIC ICC), the IEEE Wireless Communications and Networking Conference (WCNC), the IEEE Vehicular Technology Conference (VTC), and the IEEE International Symposium on Communication Systems, Networks and Digital Signal Processing (IET CSNDSP).



**RIKU JÄNTTI** received the M.Sc. degree (Hons.) in electrical engineering and the D.Sc. degree (Hons.) in automation and systems technology from the Helsinki University of Technology (TKK), in 1997 and 2001, respectively. He was a Professor pro term with the Department of Computer Science, University of Vaasa. In 2006, he joined the School of Electrical Engineering, Aalto University (formerly known as TKK), Finland, where he is currently an Associate Professor (tenured) in communications engineering and the Head of the Department of Communications and Networking. His research interests include radio resource control and optimization for machine type communications, cloud-based radio access networks, spectrum and co-existence management, and RF inference. He is an Associate Editor of the IEEE TRANSACTIONS ON VEHICULAR TECHNOLOGY. He is also an IEEE VTS Distinguished Lecturer (Class 2016).

...